Microscopic study of the giant multipole resonances in light deformed nuclei via radiative capture reactions

K. W. Schmid
Institut für Kernphysik der Kernforschungsanlage Jülich, D-5170 Jülich, West Germany

G. Do Dang
Laboratoire de Physique Théorique et Hautes Energies, Université de Paris XI, F-91405 Orsay, France*
(Received 1 November 1976)

A microscopic model for the description of the giant multipole resonances in light deformed nuclei and their excitation via (p,γ) reactions is proposed. A version of Feshbach's formalism of nuclear reactions is used for which the bound states of the target and compound systems are described as linear combinations of angular momentum projected deformed hole and particle-hole configurations, respectively. The theory is applied to study the giant multipole resonances in ^{20}Ne as seen via ^{19}F$(p,\gamma)^{20}$Ne reactions. Results for both the transitions to the ground state as well as the first 2^+ excited state of ^{20}Ne are calculated and a number of approximations are tested. The 90° yields are found to be in good agreement with experiment. Gross features as well as intermediate structures of the experimental cross sections are reasonably well reproduced.

NUCLEAR STRUCTURE ^{19}F, ^{19}Ne, ^{20}Ne; Calculated spectra and $E1$ transitions. Angular momentum projected Hartree-Fock and Tamm-Dancoff methods.

NUCLEAR REACTIONS ^{19}F(p,γ); radiative capture. Calculated cross sections to ground and first excited state.

I. INTRODUCTION

During the last 15 years, the proton radiative capture reaction has been well established as a useful tool for the experimental study of the giant multipole resonances (GMR) in nuclei.[1-11] Within the same period, some microscopic theories of photonuclear as well as particle scattering processes have been developed and used to study these resonances with some success.[8,12-27] However, while both the microscopic structure as well as the excitation mechanism of the GMR for a couple of spherical nuclei seem to have been reasonably well understood, there have been only few attempts[22,28-30] to tackle the problem in deformed nuclei. For the latter, the (p,γ) experimental data[5,6] display some very interesting features from which one may hope to extract some information about the GMR, in addition to what one can learn from the spherical case. For example, the (p,γ) excitation functions for deformed nuclei show more structures than for spherical ones. Furthermore, in addition to the (p,γ_0) decay to the ground state, transitions leading to the low-lying first excited 2^+ states have also been measured. These (p,γ_1) cross sections are found to be of the same order of magnitude as, and in some cases, even larger than, the corresponding (p,γ_0) ones, and their angular distributions are usually quite different.

The above features can be understood from the phenomenological point of view. The hydrodynamical model[31] predicts a splitting of the GMR in deformed nuclei corresponding to the various possible angular momentum projections on the symmetry axis. Such splittings have been observed experimentally in various nuclei of the rare earth region.[32] Furthermore, some of the additional structures of the excitation functions may be interpreted with the help of the rotational model.[33] In deformed nuclei, we expect rotational bands on the ground state as well as on excited states. Because of the similar intrinsic structure of the states within a band and of the different angular momentum selection rules for the transitions involved, this would explain why the (p,γ_0) and the (p,γ_1) cross sections are of comparable magnitude but their angular distributions are quite different.

The essential difficulty for a microscopic treatment of the GMR in deformed nuclei is the creation and handling of suitable many-nucleon wave functions. In spherical nuclei, the relevant many-nucleon configurations, namely the 1p-1h, or even the 2p-2h and 3p-3h configurations, can be, without much labor, coupled to definite angular momenta. The continuum is then incorporated, either directly as in the continuum shell-model calculations,[34] or indirectly as in Feshbach's formalism[35] or R-matrix theory.[36] In deformed nuclei, on the other hand, neither the Hartree-Fock (HF) de-

terminant nor the particle-hole configurations have definite angular momenta. Hence, apart from the cases where shell-model wave functions are available,[22] or where the deformation has simply been neglected,[29] one either has to forget about the continuum and to be content with a description of the nuclear structure (bound state) part of the GMR in terms of intrinsic Tamm-Dancoff (TD) or random-phase approximation (RPA) wave functions,[30] or one is forced to perform numerically complicated angular momentum projections.

The first attempt to use angular momentum projected deformed wave functions in (p,γ) and (p,n) reactions on light nuclei has been made by Afnan.[28] Using Feshbach's formalism, he first defines the basis of bound state wave functions by performing a diagonalization of the total Hamiltonian in the space of very limited 1p-1h configurations. The resulting intrinsic wave functions are then projected to good total spin by using the limit of strong deformations.[33] This probably is the reason, since such a limit is hardly justifiable for light nuclei, for the rather poor agreement of his results, at least as far as the GMR part is concerned, with experimental data.

It is the purpose of this work to make a careful study of the (p,γ) reactions on deformed nuclei with excitation of the GMR. For this purpose, a version[21] of the Feshbach formalism has been adopted. We pay special attention to the definition of the bound state wave functions for which a model has been proposed earlier.[37] In the projected Tamm-Dancoff (PTD) model, the bound states of the target (odd-mass) and compound (even-mass) systems are defined as linear combinations of angular momentum projected states of hole and particle-hole configurations relative to the Hartree-Fock intrinsic state. The problem of the center-of-mass spuriousity is dealt with approximately by the method of Elliot and Skyrme.[38]

In the next section, after a sketch of the reaction formalism, we give a careful description of how the different configuration spaces are being defined and, using these, how the T matrix of the reaction can be calculated. Section IV deals with the application of the model to the study of the $^{19}\mathrm{F}(p,\gamma)^{20}\mathrm{Ne}$ reaction. Different approximations, some of which are usually used in the literature, are tested and the results are compared with experiment whenever available.

II. REACTION FORMALISM AND CONFIGURATION SPACES

A. T matrix for photonuclear reactions

The T matrix for photon-induced reactions is given in first order perturbation theory by

$$T=\langle\Psi^{(-)}|H_\gamma|I\rangle . \tag{1}$$

Here, $|I\rangle$ is the initial state of the target nucleus and H_γ the electromagnetic interaction. The final state $|\Psi^{(-)}\rangle$ is an eigenstate of the nuclear Hamiltonian H

$$(E-H)|\Psi^{(-)}\rangle=0 \tag{2}$$

and has to fulfil the proper boundary conditions for the exit channel under consideration. In the following, we shall be interested only in single-nucleon emission processes to a limited number of open channels. All other channels will be treated only indirectly.

A convenient method, at least for our problem, to calculate the T matrix is provided by Feshbach's projection operator formalism[35] which allows a transparent classification of the states of the nuclear Hilbert space according to their configurations. We shall use in the following a version of this formalism, designed by Wang and Shakin[21] specifically to study photonuclear reactions. The total Hilbert space is divided into three orthogonal subspaces P, d, and x, using the notations of Ref. 21. The continuum space P contains all the configurations formed by one nucleon in the continuum coupled to all those states of the $(A-1)$ nucleon (odd-mass) system which are going to be treated explicitly. The photon reaction is supposed to go through a set of selected states of the compound (even) system which form the "doorway" space d. Finally, the rest of the Hilbert space is collected in the x space which is supposed to have only a marginal influence on the reaction being considered.

Let $|c^{(-)}\rangle$ be an exit channel belonging to the P space, the T matrix leading to this channel is given, using standard techniques, by

$$T=\langle c^{(-)}|\mathcal{H}_\gamma|I\rangle+\langle c^{(-)}|\mathcal{H}_{Pd}(E-\mathcal{H}_{dd}-\mathcal{H}_{dP}G_P^{(+)}\mathcal{H}_{Pd})^{-1}\times(1+\mathcal{H}_{dP}G_P^{(+)})\mathcal{H}_\gamma|I\rangle , \tag{3}$$

where the "effective" nuclear and electromagnetic interactions are defined as

$$\mathcal{H}=H+H\frac{x}{E-H_{xx}}H \tag{4}$$

and

$$\mathcal{H}_\gamma=H_\gamma+H\frac{x}{E-H_{xx}}H_\gamma . \tag{5}$$

In this way, the continuum space is defined by some effective Hamiltonian $\mathcal{H}_{PP}$,

$$(E-\mathcal{H}_{PP})|c^{(-)}\rangle=0 , \tag{6}$$

in terms of which the Green's function $G_P^{(+)}$ is given by

$$G_P^{(+)}=(E-\mathcal{H}_{PP}+i\epsilon)^{-1} . \tag{7}$$

Of course, one has not gone any farther because

Eq. (3) is a formal exact expression involving very complicated operators and as such cannot be used directly for practical calculations. In order to make the expression tractable, a number of approximations and assumptions is needed. First, let us define, inside of the doorway space, a set of configurations of H_{dd}

$$(E_d - H_{dd})|d\rangle = 0 . \tag{8}$$

Next, following Wang and Shakin, we assume that the states of the x space cannot be reached directly from $|I\rangle$ by the electromagnetic interaction

$$\langle \Psi^{(-)}|xH_\gamma|I\rangle = 0 \tag{9}$$

and, furthermore, that they are not connected to the P space through the nuclear interaction

$$\langle \Psi^{(-)}|PHx|\Psi^{(-)}\rangle = 0 . \tag{10}$$

Left to be considered is the doorway-doorway coupling via the x space which should take care of the following two effects. First, it should describe the so-called "spreading width" resulting from the coupling of the doorway states to more complicated bound A-nucleon configurations and second, it should take into account the absorption due to those channels $|c^-\rangle$ of Eq. (6) which are not explicitly included in the calculations.

The spreading width is obviously strongly dependent on the actual choice of the doorway space. As can be seen in the following section we shall use as doorway states all the possible linear combinations of angular momentum projected deformed 1p-1h states with respect to the deformed A nucleon Hartree-Fock determinant. Since these wave functions are, expressed in terms of shell-model configurations with respect to a spherical reference state, very complicated superpositions of 1p-1h, 2p-2h, and many particle-many hole states, our d space includes much more degrees of freedom than are usually taken into account considering spherical nuclei. Hence here the spreading will be much less important than in the latter ones and could perhaps, in a not too bad approximation, even be neglected.

The additional absorption due to the neglected channels could naturally be described by choosing a complex optical potential for the scattering waves. Then, if the spreading width is small, the introduction of an x space would be unnecessary. However, we are going to use only real potentials and have hence to try to include this additional absorption via the x space.

Because we know nothing more than just mentioned above about the x space and can hence hardly do anything better, we shall in the following approximate the doorway to doorway coupling via the x space as in Ref. 21 by a diagonal energy independent constant

$$\langle d|Hd_x(E - H_{xx})^{-1}H_x d|d'\rangle \approx \delta(d,d')(\Delta_x - i\Gamma_{x/2}) . \tag{11}$$

We would like to point out that the values $\Delta_x = 0$ and $\Gamma_x = 150$ keV which we have used are very small compared to, for example, the two additional width of both 400 keV introduced in Ref. 21, and that we have therefore good reason to hope that the approximation (11) does not do too much harm to our final results. With the above approximations, the T matrix of Eq. (4) can be rewritten as

$$T^{(\gamma)}_{c,I} = \langle c^{(-)}|H_\gamma|I\rangle + \sum_{dd'} \langle c^{(-)}|H_{Pd}|d\rangle M^{-1}_{dd'} \times (\langle d'|H_\gamma|I\rangle + F^{(\gamma)}_{d',I}) , \tag{12}$$

where the "initial state interaction" term $F^{(\gamma)}_{d',I}$ is given by

$$F^{(\gamma)}_{d',I} = \langle d'|H_{dP}G^{(+)}_P H_\gamma|I\rangle \tag{13}$$

and the "shift and width" matrix M by

$$M_{dd'} = \delta(d,d')[E - E_d - \Delta_x + \tfrac{1}{2}i\Gamma_x] - \langle d|H_{dP}G^{(+)}_P H_{Pd}|d'\rangle . \tag{14}$$

The T matrix of Eq. (12) has been derived for the (γ,p) reactions. Because of the interest in the inverse process, the radiative capture, the complex conjugate of Eq. (12) has to be used. Then, $|c^{(+)}\rangle$ describes the ground state of the target plus the incoming nucleon and $|I\rangle$ the final state of the A nucleon system. Furthermore, $F^{(\gamma)}_{d,I}$ has to be interpreted as the "final state interaction" term.

Equation (12) is the central result of this section. Its calculation requires the knowledge of the wave functions of the nuclear systems in the d and P spaces. This is what will be given in the following sections.

B. Bound states of the target and compound systems

There are two classes of bound states: the bound states of the A-nucleon system, namely the final nuclear states or the doorway states, and those of the target nucleus which are to be coupled to the scattering waves to form the P space. To define these states, we shall use a version of a model proposed recently,[37] namely the angular momentum projected Tamm-Dancoff model. As it has already been explained in detail, we shall sketch below only the main lines.

As usual, the theory starts by giving a set of spherical single-particle wave functions which we denote by the indices $a, b, c, \ldots$. We assume that, inside of this model space, the total Hamiltonian

can be written as a sum of a kinetic and a two-body interaction term:

$$H=\sum_{ab} t(ab)c_a^\dagger c_b+\tfrac{1}{4}\sum_{abcd} V(abcd)c_a^\dagger c_b^\dagger c_d c_c\,. \tag{15}$$

Recalling that we are dealing with deformed nuclei, our first task is to define the average deformed field and the corresponding single-particle orbitals. Using the Hartree-Fock theory,[39] the orbitals, which we shall denote by the indices $i,k,j,\ldots$, can be expressed as

$$a_i^\dagger=\sum_a A_{ai}c_a^\dagger, \tag{16}$$

where the variational parameters A_{ai} can be obtained in the usual way by minimizing the expectation value of the Hamiltonian in the reference state in which the nucleons occupy the lowest orbitals, up to some level F. This is the unperturbed Hartree-Fock state $|\,\rangle$ and any excitation of the system in this intrinsic frame can be viewed as a creation of particles and holes across the surface F. A set of such excitations which will play a very important role in our problem is composed of one particle-one hole excitations

$$|M\alpha^{-1}\rangle=a_M^\dagger a_\alpha|\,\rangle\,. \tag{17}$$

Now, for $N=Z$ nuclei, if we do not allow any parity and isospin mixing (neglecting the Coulomb force) in the expansion (16), then the Hartree-Fock state will have positive parity and $T=T_z=0$. Furthermore, if we assume axial symmetry, as we do in the following, the reference state will in addition have a definite angular momentum projection $K=0$ on the symmetry axis and is even under time reversal. Also in the limits of the above assumptions, the particle-hole states can be coupled to good isospin and, by making linear combinations, can be made to have definite properties under parity and time reversal operations. Of course, the above states do not correspond to any definite total angular momentum. In order to use them in our calculations, we must first project them to good total spin: this can be done by using Villars's projection operator[40]

$$P^{JM}=\frac{2J+1}{8\pi^2}\int d\Omega D^{J*}_{KM}(\Omega)\hat{R}(\Omega)\,, \tag{18}$$

where $\hat{R}(\Omega)$ is the rotation operator and $D^J_{KM}(\Omega)$ the rotation matrix. Actually, because of the assumed axial symmetry, the integral in Eq. (18) can always be reduced to a single integral involving only one polar angle, Θ. The overlap function of the reference state, for example, is given simply by

$$\langle\,|\hat{R}(\Omega)|\,\rangle=\det|X_{ik}(\Theta)|\quad i,k\le F\,, \tag{19}$$

with

$$X_{ik}(\Theta)=\langle i|\hat{R}(\Omega)|k\rangle=\sum_{ab}A_{ai}\langle a|\hat{R}(\Theta)|b\rangle A_{bk}\,. \tag{20}$$

Starting from the reference state and the set of particle-hole states coupled to good isospin, the projection operator allows one to define the following basis states with total angular momentum J, parity π, and isospin T:

$$\begin{aligned}&\text{From } |\,\rangle:\\ &\quad |J^\pi M_J T=0\rangle=P^{JM}|\,\rangle\,;\\ &\text{From } |M\alpha^{-1}\rangle:\\ &|[M\alpha^{-1}]J^\pi M_J T\rangle\\ &\quad=P^{JM}\frac{1}{\sqrt{2}}\{[a_M^\dagger a_\alpha|\,\rangle]_T+\pi(-1)^{J-(m_M-m_\alpha)}[a_{\bar{M}}^\dagger a_{\bar{\alpha}}|\,\rangle]_T\}\,,\end{aligned} \tag{21}$$

where $\bar{M}$ and $\bar{\alpha}$ indicate the time-reversed states of M,α.[41] Because of the angular momentum projection, this basis is not orthogonal even though the states of the intrinsic system are. As a consequence, to define the states of the A-nucleon system, a diagonalization of the total Hamiltonian will lead to equations of the form

$$(H^{J^\pi T}-E^{J^\pi T}N^{J^\pi T})C^{J^\pi T}=0\,, \tag{22}$$

where $H^{J^\pi T}$ and $N^{J^\pi T}$ are the energy and overlap matrices, respectively, for states with quantum numbers $J^\pi T$. Note that, in this way, the projected ground state is no longer just the one obtained from $|\,\rangle$: it also contains components coming from the particle-hole basis with the same quantum numbers. This is equivalent to an approximate projection before variation for the average field which has been assumed to be the same for all the intrinsic states under consideration, an assumption which had been shown to be quite good[37] at least as far as negative parity states are concerned.

Now, it is well known that states such as Eq. (21) obtained by exciting particle-hole pairs across shells may contain spurious components coming from the center-of-mass motion.[38] While in spherical nuclei, the spurious state can either be explicitly constructed and projected out[42] or overcome by the use of the random-phase approximation,[43] the problem is much more complicated in deformed nuclei. Here, an explicit construction of the spurious state is practically impossible and the RPA cannot be used mostly because the behavior of its ground state under rotation is not known. We therefore adopt an approximate method proposed by Elliot and Skyrme[38] to eliminate the center-of-mass spuriousity: it consists simply in a diagonalization of the operator $(1/A)\vec{R}_{\text{c.m.}}{}^2$ in the

basis being considered. Had our basis states been complete and defined by the use of harmonic oscillator wave functions, the diagonalization would have given rise to a number of states with eigenvalues $\frac{3}{2}b^2$ which are nonspurious and others with eigenvalues $\frac{5}{2}b^2$, $\frac{7}{2}b^2$, ... which are spurious. Actually, because our basis is mostly incomplete, the eigenvalues are expected to come out close to the above values.[42] We then consider all states with eigenvalues near $\frac{3}{2}b^2$ as nonspurious and project out all others with eigenvalues around $\frac{5}{2}b^2$ or above. In this way, the spurious components in the basis states (21) are, at least partially, eliminated.

Left to be considered in this section is the problem of the bound states of the target nucleus. This will be done as follows. Starting from the Hartree-Fock state $|\rangle$ of the A-nucleon system, we form a set of hole states $a_\alpha|\rangle$. Using the projection (18), a basis of states with total angular momentum I, parity π is given by

$$|\alpha^{-1} I^\pi M_I\rangle = P^{IM_I}\frac{1}{\sqrt{2}}(a_\alpha|\rangle + \pi(-1)^{I+m_\alpha} a_{\bar{\alpha}}|\rangle), \tag{23}$$

where again $\bar{\alpha}$ is the time-reversed state of α. The bound states of the target nucleus are then obtained by a diagonalization of the total Hamiltonian in the basis (23). As in the case of the A-nucleon system, this basis is not orthogonal and one is led again to eigenvalue equations of the form (22). The calculations of the various matrix elements of the Hamiltonian and the overlap functions are straightforward even though at places they become rather lengthy due to the angular momentum projection.

C. Continuum states

These states are supposed to be given by coupling the scattering waves of the incident particle to the bound states of the target nucleus. To treat these states properly, we shall follow the prescription of Wang and Shakin[21] based on the work of Auerbach *et al.*[44]

One first defines a preliminary channel vector by

$$|r,c\rangle = \sum_{M_I m_c} \langle I j_c M_I m_c | J_c M_c\rangle b_c^\dagger(r)|I^\pi M_I\rangle, \tag{24}$$

where $|I^\pi M_I\rangle$ is one of the hole states defined in the previous section and $b_c^\dagger(r)$ is the creation operator of a particle with the quantum number $c \equiv (l_c j_c m_c \tau_c)$ at the distance r. Such a channel vector is clearly not orthogonal to the states of the d space because the $b^\dagger(r)$ operator can create a nucleon in a bound orbital. We shall see later how to orthogonalize the two spaces. Let us first say a few words about the scattering waves. They are defined by some effective Hamiltonian $h_c(r)$ which is supposed to be local and furthermore to be diagonal in the channel indices (i.e., we neglect channel coupling). As usual, this Hamiltonian is then taken to be some optical potential $U_c(r)$, e.g., a Woods-Saxon potential. The radial part of the scattering waves is of the form $\tilde{v}_c^{E(\pm)}(r) = \exp[\pm i\delta_c(E)]\tilde{v}_c^E(r)$, where $\delta_c(E)$ is the phase shift of the indicated channel and $\tilde{v}_c^E(r)$ is the solution of the Schrödinger equation

$$\left[\frac{d^2}{dr^2} - \frac{l_c(l_c+1)}{r^2} - U_c(r) - k^2\right]\tilde{v}_c^E(r) = 0 \tag{25}$$

with $E = k^2/2m$. In this way, the Green's function is given by

$$g_c^{E(\pm)}(r,r') = -\pi\tilde{v}_c^E(r_<)[\tilde{w}_c^E(r_>) \pm i\tilde{v}(r_>)], \tag{26}$$

where $\tilde{w}_c^E(r)$ is the irregular solution of Eq. (25).

Now, a preliminary channel state can be defined as

$$|\tilde{c}^{(\pm)}\rangle = \int_0^\infty \frac{\tilde{v}_c^{E(\pm)}(r)}{r}|r,c\rangle r^2 dr\,. \tag{27}$$

From the above, it becomes obvious how to orthogonalize the space spanned by the channel vectors (24) to the d space. In the case where the bound state orbitals are already orthogonal to the scattering waves, e.g. if they are all solutions of the same optical potential, this can be done by defining new channel vectors by

$$|r,c\rangle = (I - \sum_b |b\rangle\langle b|)|r,c), \tag{28}$$

using the notations of Ref. 21 where b runs over all bound states (occupied or not) with the same quantum numbers as those of the scattering waves. Using Eq. (28) instead of Eq. (24) will not modify the wave functions $\tilde{v}_c^E(r)$ but leads to an additional term in the Green's function.

Instead of considering a modification of the channel vectors, one can equally stick to the original definition (24) and treat the orthogonalization in terms of modified scattering waves and Green's functions. Let us define a projection operator Q_c by

$$Q_c f(r) = f(r) - \sum_b R_b(r)\langle b|f\rangle \tag{29}$$

with $f(r)$ being any well-behaved function. It is then obvious that with the definitions (24) and (27) for the channel states and the following modified functions

$$v_c^E(r) = Q_c\tilde{v}_c^E(r) \tag{30}$$

$$g_c^{E(+)}(r,r') = Q_c\tilde{g}_c^{E(+)}(r,r') \tag{31}$$

one would get exactly the results of Ref. 21. The advantage of this prescription consists in the fact that it can be used even when the bound single-

particle states are not eigenstates of $h_c(r)$. One then simply has to change Q_c: As a matter of fact, it has been shown[45] that any arbitrary state $|b\rangle$ can be eliminated from the spectrum of eigenstates of Eq. (25) by using the projection operator

$$Q_c = I - \tilde{g}_c^{E(+)} \frac{|b\rangle\langle b|}{\langle b|\tilde{g}_c^{E(+)}|b\rangle} \tag{32}$$

instead of what is given by Eq. (29). The generalization to the case where more than one state with the same quantum numbers have to be eliminated is straightforward.

The essential approximation made in this section is the neglect of the channel-channel coupling. This approximation is supposed to be reasonable if there is no single-particle resonance in the scattering waves. However, if such a resonance appears, one can always extract from its wave function a quasibound state which can then be included in the d space and projected out from the P space by the prescription (32).[45] The remaining spectrum will not contain this resonance any more.

In the following, we shall always use the modified wave and Green's functions defined by Eqs. (30) and (31) with Q_c given by Eq. (32). A channel state is thus

$$|c^{(\pm)}\rangle = \int_0^\infty \frac{v_c^{E(\pm)}(r)}{t} |r, c\rangle r^2 dr\,, \tag{33}$$

where $v_c^E(r)$ is given by Eq. (30) and may have been modified by possibly appearing resonances.

D. Continuum-bound state coupling and the differential cross section

We can now proceed to calculate the different terms of the T matrix involving a coupling of the bound states Eq. (21) to the continuum channel states of the last section. Let us consider first the term $\langle c^{(-)}|H_\gamma|I\rangle$ representing the "direct" part of the radiative capture process. For the electromagnetic interaction, we shall use the electric multipole operators $\hat{Q}^L$ of the long wave length limit

$$\hat{Q}_\nu^L = \sum_{ab} q_\nu^L(ab) c_a^+ c_b\,, \tag{34}$$

where

$$q_\nu^L(ab) = \omega_\nu^L(ab) \int_0^\infty r^2 dr\, R_a(r) r^L R_b(r)\,, \tag{35}$$

$$\omega_\nu^L(ab) = e_{\text{eff}}^a \delta(\tau_a, \tau_b) \tfrac{1}{2}[1 + (-1)^{l_a + l_b + L}] (-1)^L \left(\frac{2L+1}{4\pi}\right)^{1/2}$$

$$\times \langle j_a L \tfrac{1}{2} 0 | j_b \tfrac{1}{2}\rangle \langle j_b L m_b \nu | j_a m_a\rangle\,. \tag{36}$$

The reduced matrix element of $\hat{Q}^L$ between a continuum channel state (33) and a state of the ground state band can be written as

$$\langle c^{(-)} \| \hat{Q}^L \| I\rangle = e^{i\delta_c(E)} \int_0^\infty r^2 dr \frac{v_c^E(r)}{r} f_{c,I}^L(r)\,. \tag{37}$$

Here, $f_{c,I}^L(r)$ is the form factor

$$f_{c,I}^L(r) = (r, c \| \hat{Q}^L \| I\rangle = r^L \sum_b R_b(r) \Omega_{c,I}^b(L)\,, \tag{38}$$

where in $\Omega_{c,I}^b(L)$ we collect all the factors which come from the angular momentum coupling and the integration over the rotation angle Θ. The angular momentum coupling part is most straightforward and as to the part coming from the angular momentum projection, it can be handled by the usual techniques[40] exactly in the same way as for the calculation of the overlap and energy matrices of Sec. II B. The use of the primitive channel vector (24) in Eq. (37) instead of the orthogonalized one, Eq. (28), is compensated by the fact that the orthogonalization is already taken into account by the replacement of $\tilde{v}_c^E(r)$ by the modified scattering wave $v_c^E(r)$. Furthermore, the summation over b in Eq. (38) runs over all bound single-particle states of the d space. In a similar way, the coupling between the P and d spaces via the nuclear interaction H_{Pd} can be calculated. One obtains

$$\langle c^{(-)}|H_{Pd}|d\rangle = e^{i\delta_c(E)} \int_0^\infty r^2 dr \frac{v_c^E(r)}{r} F_{c,d}(r)\,. \tag{39}$$

For a δ interaction, the form factor $F_{c,d}(r)$ can be written as

$$F_{c,d}(r) = (r, c|H_{Pd}|d\rangle = \sum_{abe} R_a(r) R_b(r) R_e(r) \Lambda_{c,d}^{abe}\,, \tag{40}$$

where again, $\Lambda_{c,d}^{abe}$ contains all the factors coming from the angular momentum coupling and integration over Θ. Using the above formulas, together with Eq. (31), one gets for the shift and width matrix, Eq. (14), the contribution

$$\langle d|H_{dP} G_P^{(+)} H_{Pd}|d'\rangle = \sum_c \iint dr\, dr' r F_{c,d}(r) g_c^{E(+)}(r, r') F_{c,d'}(r') r' \tag{41}$$

and for the final state interaction term

$$\langle d \| H_{dP} G_P^{(+)} \hat{Q}^L \| I \rangle = \sum_c \iint dr\, dr'\, r F_{cd}(r) g_c^{E(+)}(r,r') f_{c,I}^L(r') r' \,. \tag{42}$$

In the above equations, the sums run over all channels c included in the calculation.

We now have all the ingredients for the evaluation of the T matrix. From this, the cross section for the radiative process (N,γ) leading from a target hole state $h=(I^\pi \tau_h \pi_h)$ to a final state J_0 of the ground state band of the A-nucleon system can be derived. It is explicitly given by

$$\frac{d\sigma(N,\gamma)}{d\Omega} = \left(\frac{2\pi}{c}\right)^2 e^2 \frac{k_\gamma}{k_N} \frac{1}{2(2I+1)} \sum_{c'LL'Qc} i^{L-L'+l_c'-l_c} A_L A_{L'} (-1)^{J_c-J_0+I+|J_c'+1+1/2-Q}$$

$$\times \frac{1}{4\pi} [(2l_c+1)(2l_c'+1)(2j_c+1)(2j_c'+1)(2J_c+1)(2J_c'+1)]^{1/2}$$

$$\times \begin{Bmatrix} j_c & l_c & \frac{1}{2} \\ l_c' & j_c' & Q \end{Bmatrix} \begin{Bmatrix} J_c & j_c & I \\ j_c' & J_c' & Q \end{Bmatrix} \begin{Bmatrix} J_c & L & J_0 \\ L' & J_c' & Q \end{Bmatrix} \langle l_c l_c' 00 | Q0 \rangle$$

$$\times \sum_{\lambda=\pm 1} (-1)^\lambda \langle L'L\lambda - \lambda | Q0 \rangle \langle [I^\pi, c] J_c \| \hat{T}^L \| J_0 \rangle \langle [I^\pi, c'] J_c' \| \hat{T}^{L'} \| J_0 \rangle^* P_Q(\hat{k}_N \cdot \hat{k}) \,, \tag{43}$$

where $\vec{k}_N$ is the momentum of the incoming nucleon and

$$A_L = \sqrt{2\pi} \left[\frac{(2L+1)(L+1)}{L} \right]^{1/2} \frac{c k_\gamma^L}{(2L+1)!!} \,. \tag{44}$$

It is common practice to write the differential cross section in the form

$$\frac{d\sigma(N,\gamma)}{d\Omega} = a_0 \left[1 + \sum_{Q \geq 1} a_Q P_Q(\cos\Theta) \right] , \tag{45}$$

from which the total cross section is given by $4\pi a_0$.

III. APPLICATION TO THE $^{19}F(p,\gamma)^{20}Ne$ REACTION

As a test of the physical approximation as well as of the numerical feasibility, we have applied the method and the model described in the previous chapters to study the multipole resonances of ^{20}Ne as seen via the $^{19}F(p,\gamma)^{20}Ne$ radiative capture reaction.

First of all, we shall suppose that the transition is mainly dipole electric so that the operator $\hat{Q}^{L=1}$ is just the electric dipole operator for which we use the effective charges $\frac{1}{2}e$ for proton and $-\frac{1}{2}e$ for neutron. We shall discuss later on possible contributions from other multipoles, in particular from quadrupole transitions. The electric dipole operator is an isospin vector and as the states of the ground state rotational band all have $T=0$, all intermediate states contributing in the process must have $T=1$, and furthermore must have negative parity. These states consequently will not contain any component from the projected Hartree-Fock determinant. We shall suppose furthermore that the ground state rotational band does not contain components from projected particle-hole configurations with the same quantum numbers, in other words it is given by simple projected Hartree-Fock states. This is known to be a good approximation for ^{20}Ne.[46] We have furthermore neglected the mixing of configurations with intrinsic odd ΔK in Eq. (22). It has been checked that this approximation has no significant effect on the negative parity states. Its effect on the positive parity states will be studied in some future work.

Because we are interested in both transitions to the ground state as well as to the first 2^+ excited state of ^{20}Ne, all intermediate states with $J^\pi = 1^-$, 2^-, or 3^- will contribute. We hence restrict the partial wave expansion of the incoming particle to the s, p, d, and f waves of the Woods-Saxon potential. The parameters of this potential are taken over without modification from Afnan.[28] They are $U_0 = -50.5$ MeV, $U_{ls} = -6.85$ MeV, and $a_0 = 0.70$ fm. Furthermore, the central, spin-orbit, and Coulomb radii have been assumed to be equal and state independent, given by $R = r_0(A-1)^{1/3}$ with $r_0 = 1.25$ fm.

As described in Sec. IIC, the channel states must be orthogonalized with respect to the bound states of the d space. As the single-particle states of this space have been taken to be described by harmonic oscillator wave functions, the orthogonalization is then carried out using the prescription (32). Only $0s$-, $0p$-, $1s0d$-, and $0f$-oscillator states have been adopted, as the p waves of the Woods-Saxon potential do not show any resonance which would permit the extraction of a quasibound state. Using this basis, together with a modified-

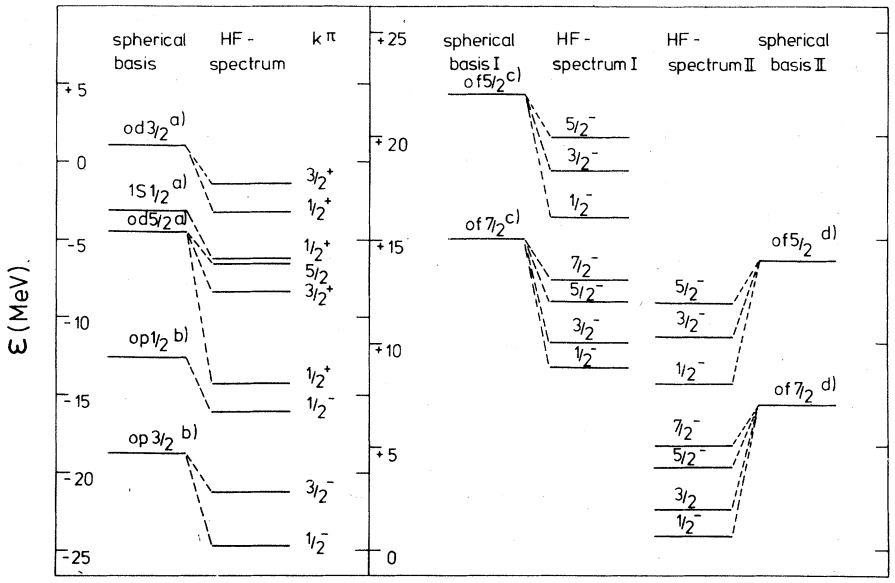

FIG. 1. The spherical single-particle energies and the resulting HF spectra: (a) Ref. 47; (b) experiment + 3 MeV; (c) Ref. 10; (d) Ref. 10 minus 8 MeV.

surface δ interaction[47] (MSDI) with parameters $A_{T=0}=0.77$ MeV, $A_{T=1}=0.95$ MeV, $B_{T=0}=-2.51$ MeV, and $B_{T=1}=0.37$ MeV as the residual interaction for the d space, the Hartree-Fock problem is then solved. For this purpose, we make the additional assumption that there is no orbital mixing between different shells and thus we can use single-particle energies relative to the unperturbed ^{16}O core. For the $1s0d$ shell, they are taken from Halbert *et al.*[47] to be $\epsilon_{d_{5/2}}=-4.49$, $\epsilon_{s_{1/2}}=-3.16$, and $\epsilon_{d_{3/2}}=+1.05$, all in MeV. For the $0p$ shell, we have adopted the values $\epsilon_{p_{3/2}}=-18.74$ MeV and $\epsilon_{p_{1/2}}=-12.6$ MeV, which are about 3 MeV higher than the experimental values in ^{16}O. This upward shift is necessary in order to reproduce roughly the right separation between the first $I^\pi=\frac{1}{2}^-$ band and the $I^\pi=\frac{1}{2}^+$ ground state band in the $A=19$ system. One may think of this as a renormalization of the effective interaction. As a matter of fact, the MSDI as used here can hardly describe the interaction between shells. The choice of the $0f$ single-particle energies is more complicated. There are some experimental as well as theoretical evidences[10] that in the neighborhood of ^{16}O, the ϵ's are at about 15 MeV and 22 MeV for the $0f_{7/2}$ and $0f_{5/2}$, respectively. However, as for the $0p$ shell, a shift from these values is possible and we have used another set with $\epsilon_{f_{7/2}}=7$ MeV and $\epsilon_{f_{5/2}}=14$ MeV, denoted below as set II. These are roughly the energies where f-wave resonances are found for the Woods-Saxon potential.

The results of our d-space calculations are summarized in Figs. 1–4. Figure 1 displays the intrinsic Hartree-Fock single-particle spectrum. The appearance of a large gap between the last occupied and the first unoccupied orbitals indicates the relative stability of the Hartree-Fock solution and thus justifies our approximation to describe the ground state band as projected Hartree-Fock states. The ground state band is compared with experiment in Fig. 2. The agreement is excellent and in fact cannot be improved much even if higher order correlations are taken into account.[46] Figure 2 also compares the experimental low-energy spectra[48] of ^{19}F and ^{19}Ne with the theoretical prediction for the $A=19$ $T=\frac{1}{2}$ system. ^{19}F and ^{19}Ne are very good mirror nuclei, which justifies the neglect of the Coulomb force in our d-space calculations. Although our calculation interchanges the positions of the $\frac{3}{2}^-$ and $\frac{5}{2}^-$ states, the agreement of both positive and negative parity states with experiment is of the same quality as for ^{20}Ne. This supports our description, Eq. (23), of the low-lying bound states of the target nucleus. All the six states shown in Fig. 2 will be used later in our calculation to define the channels c. Actually, there are 12 macrochannels because both ^{19}F and ^{19}Ne spectra are being used.

Using the Hartree-Fock spectrum of Fig. 1, one can now construct the intermediate states $|d\rangle$ of the compound system. Because of the required negative parity and $T=1$ and since, due to our approximation of $\Delta K=$ even, only configurations with either even or odd angular momentum projection

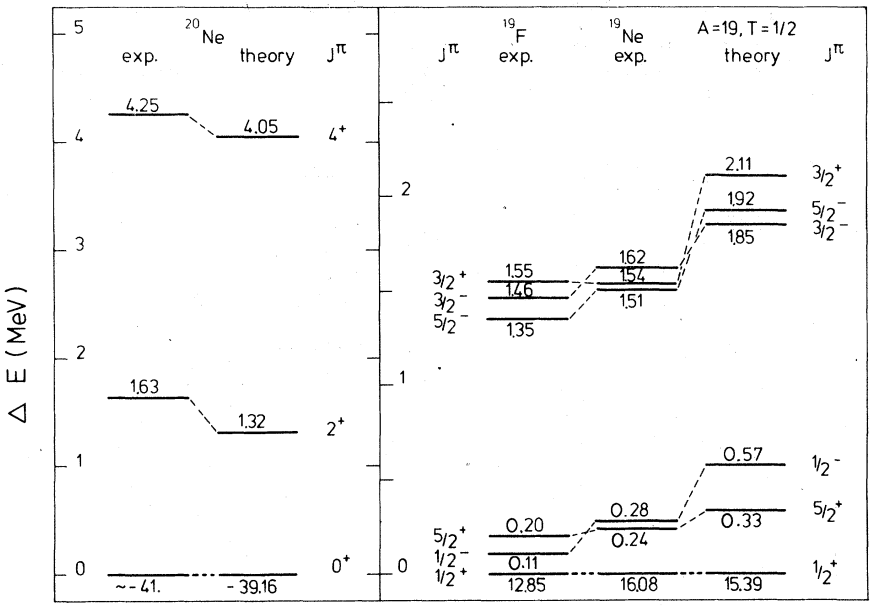

FIG. 2. The low excited bands of ^{20}Ne, ^{19}F, and ^{19}Ne.

K will mix with each other, the 1p-1h space consists of 8 and 15 configurations with even and odd K respectively, for $J^\pi = 1^-$, while the corresponding numbers are 20 and 15 for $J^\pi = 2^-$ and 20 and 22 for $J^\pi = 3^-$. Within each of the J^π sets of states thus obtained, one first solves an eigenvalue problem analogous to Eq. (22) for the center-of-mass operator $(1/A)\vec{R}^2$. All the eigenvalues found are either exactly equal or very close to the value $\frac{3}{2}b^2$. The slight deviation, of course, comes from the fact that our basis is not complete. According to Sec. II B, we may hence consider all our states as nonspurious. Note that these are $T = 1$ states. As a matter of fact, the same calculation for the $T = 0$ leads to five states with eigenvalues close to $\frac{5}{2}b^2$. (Two states for $J^\pi = 1^-$, one for $J^\pi = 2^-$, and two for $J^\pi = 3^-, T = 0$.) Figures 3 and 4 give the results obtained from the diagonalization of the Hamiltonian. Figure 3 displays the reduced $B(E1)$ values of the transitions to the ground state of ^{20}Ne, plotted against the excitation energies of the $T = 1$, $J^\pi = 1^-$ states. We distinguish the transitions coming from states built on $K = 0$ (dashed lines) and from states built on $K = 1$ (full lines). Furthermore, the results corresponding to the two sets of energies are compared. As expected from the Hartree-Fock spectrum, for Set I, the excitations from $1s0d$ to $0f$ shells are well separated from the $0p$ to $1s0d$ excitations. If Set II is used, the two excitations are seen to mix strongly with each other in the energy region between 18.5 and 23 MeV. Of course, from the bound spectra given here, one cannot say which set should be used. We shall come back to this point later. Figure 4 shows the reduced $B(E1)$ for transitions to the first excited 2^+ state. Here, all intermediate states with $J^\pi = 1^-$ (dotted lines), $J^\pi = 2^-$ (dashed lines), and $J^\pi = 3^-$ (full lines) contribute. As a result, one sees much more structures than for the ground state transitions. We observe again the same characteristics about configuration mixing depending on whether Set I or Set II is being used. It is remarkable that most of the transition strengths to the 2^+ state come from the 2^- and 3^-, but not from the 1^- states, a fact which already explains the large discrepancies between the (p, γ_0) and (p, γ_1) angular distributions. We now proceed to calculate the T matrix, as explained in Sec. II D. For this purpose, we have adopted for the residual interaction H_{Pd} a δ force with the parameters given by Wang and Shakin,[21] namely $V_0 = 613$ MeV fm^3, $a = 0.865$, and $b = 0.135$. On the other hand, the coupling of the d space to the complicated x space, as mentioned already in Sec. II A, is supposed to be state independent and diagonal in the d space. It is characterized by the parameters Δ_x and Γ_x which we shall take to be 0 and 150 keV, respectively.

With the above parameters, we have calculated the 90° yields for both the (p, γ_0) and (p, γ_1) reactions. We have taken this occasion to test a number of approximations which are often made in the literature. First of all, the final state interaction (FSI) which, to our knowledge, had never been ex-

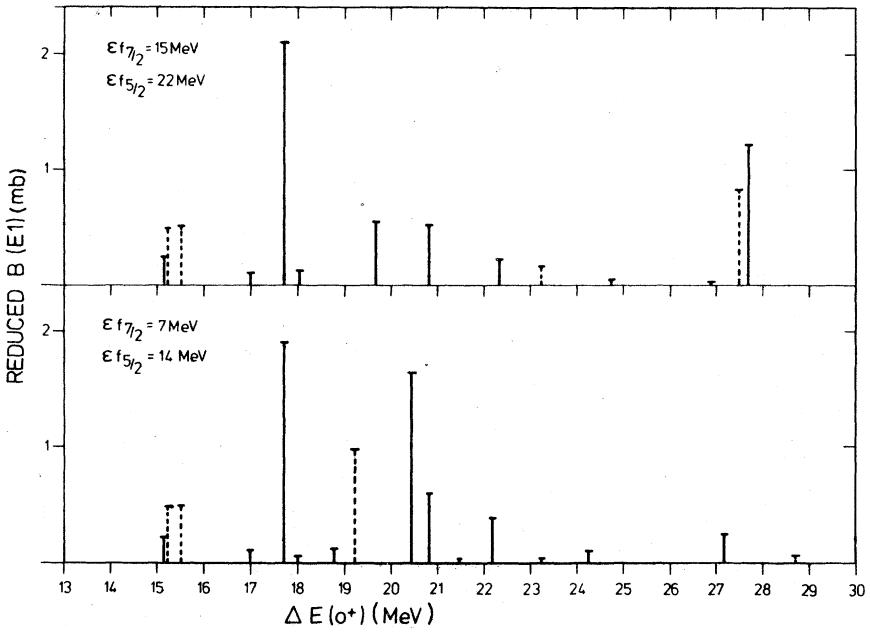

FIG. 3. The reduced $B(E1)$ values for the transitions from $T=1$, $J^\pi=1^-$ excited states to the ground state of ^{20}Ne. Dashed line: $K=0$; solid line: $|K|=1$.

plicitly calculated, has been found, at least with our model space, to be negligible. We have also examined the validity of the isolated resonance approximation (IRA) where the width and shift matrix is supposed to be diagonal in the d space, as compared to the full calculation, the matrix inversion approximation (MIA), where this matrix is effectively inverted as shown in Eq. (12). The results of the calculation are shown in Figs. 5–12 and in Table I.

Figures 5 and 6 display the 90° yields for the (p,γ_0) and (p,γ_1) reactions as calculated in the isolated resonance approximation, with the final state interaction taken into account (IRA + FSI). In

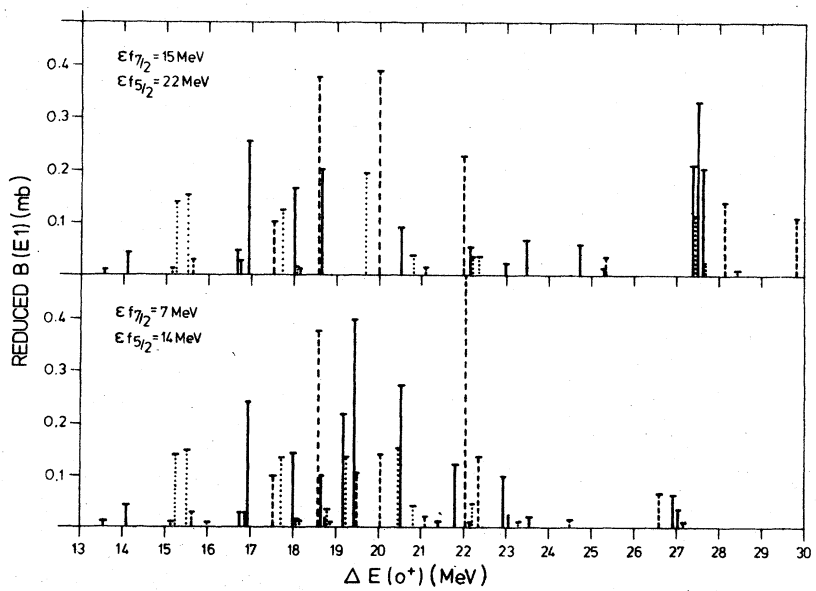

FIG. 4. The reduced $B(E1)$ values for the transitions from $T=1$ excited states to the 2^+ member of the ^{20}Ne ground-state band. Dotted line: $J^\pi=1^-$; dashed line: $J^\pi=2^-$; solid line: $J^\pi=3^-$.

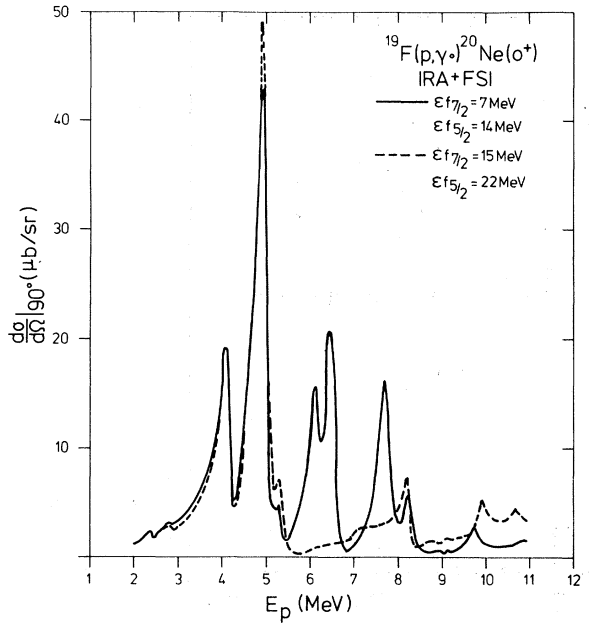

FIG. 5. The 90° yield for the $^{19}F(p,\gamma_0)^{20}Ne$ reaction as obtained for the different sets of $0f$-single-particle energies in the IRA + FSI approximation. Dashed line: Set I; solid line: Set II.

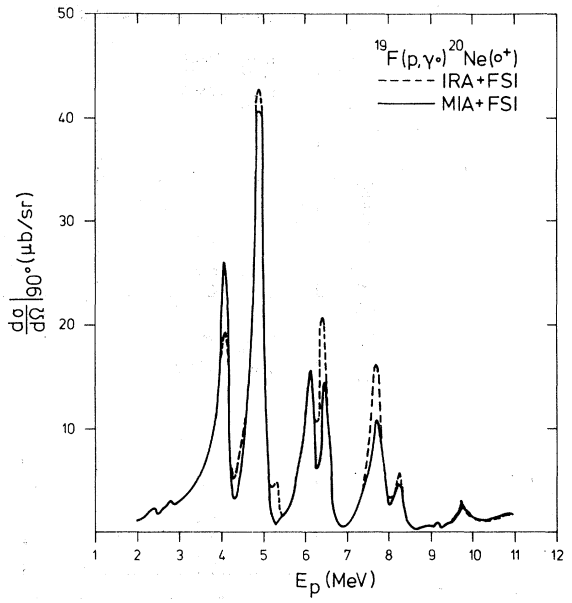

FIG. 7. Comparison of the results of a complete calculation (MIA + FSI) with those of IRA + FSI approximation for the $^{19}F(p,\gamma_0)^{20}Ne$ reaction. Set II single-particle energies are used.

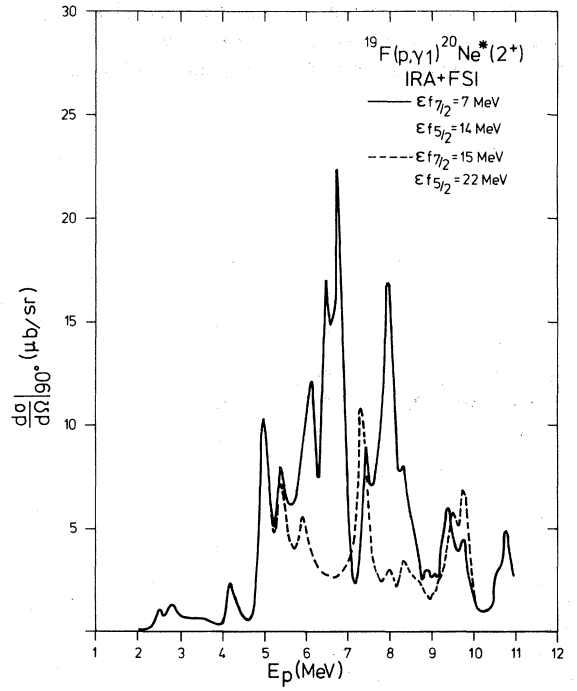

FIG. 6. Same as Fig. 5, but for the $^{19}F(p,\gamma_1)^{20}Ne^*$ (2^+) reaction.

both figures, the results obtained by using the two sets of $0f$ energies are compared with each other. While below 5.5 MeV and above 8.5 MeV incident proton energies both sets give almost identical results, one observes that Set II gives much more strengths in the region in between the above energies. We also wish to point out that the two states at 19.7 and 20.8 MeV in the bound state calculation using Set I (Fig. 3) are suppressed when connected to the continuum.

Figures 7 and 8 compare the cross section in the IRA + FSI with the results of the full calculation MIA + FSI, using Set II. In the case of the (p,γ_0) reaction (Fig. 7), only a slight redistribution of the strengths due to the matrix inversion is obtained. This is to be expected since the 1^- states of Fig. 3 are rather well separated from each other. The situation is quite different for the (p,γ_1) reaction (Fig. 8). As expected from the higher density of 2^- and 3^- states (Fig. 4), here the effect of the nondiagonal part of the width and shift matrix becomes important, leading to marked differences between the two approximations. In other words, the IRA is not valid in this case.

The results of the full calculation (MIA + FSI) using Set II are compared with the experimental results[6] in Figs. 9 and 10. The agreement should be considered as excellent, especially for the (p,γ_0) reaction, having in mind the fact that we are doing a fully microscopic calculation. Most

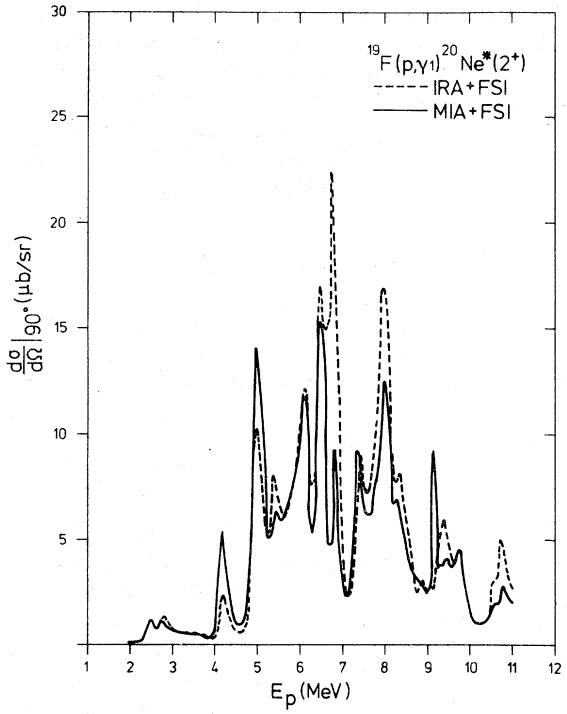

FIG. 8. Same as Fig. 7, but for the $^{19}F(p,\gamma_1)^{20}Ne^*$ (2^+) reaction.

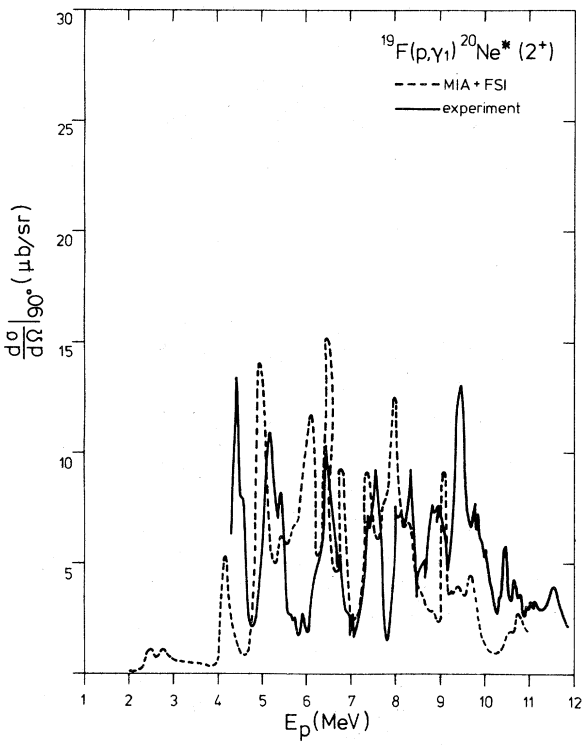

FIG. 10. Same as in Fig. 9 but for the $^{19}F(p,\gamma_1)^{20}Ne^*$ (2^+) reaction.

of the structures are reproduced including their abundance in the (p,γ_1) reaction. Of course, we do not expect to get exactly the positions of the various peaks. This would require a more careful choice of the single-particle energies as well as of the residual interactions. Furthermore, the limitation to only dipole transition is probably not satisfying. Figure 11 shows the a_2 coefficients of the (p,γ_0) and (p,γ_1) angular distributions, as defined in Eq. (45). While the agreement of the coefficient for the (p,γ_0) reaction with experiment

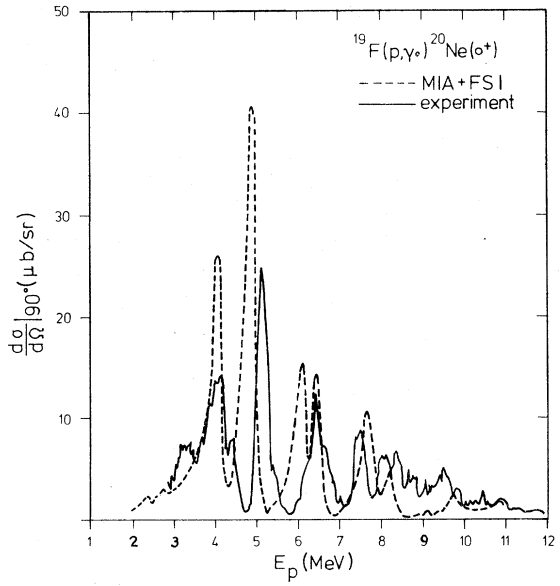

FIG. 9. Comparison of the MIA + FSI results with the experimental data for the $^{19}F(p,\gamma_0)^{20}Ne$ reaction.

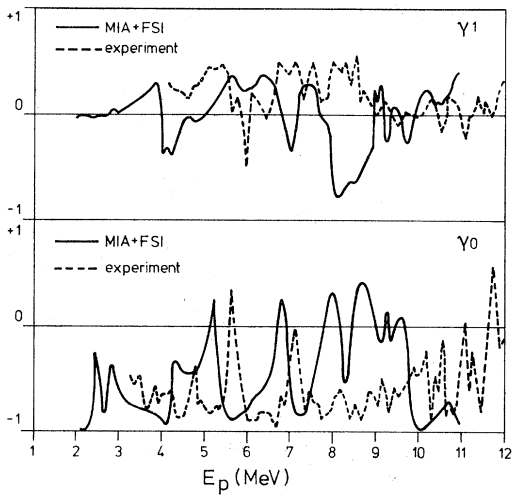

FIG. 11. Comparison of the experimental with the theoretical (MIA + FSI) a_2 coefficient of the angular distributions.

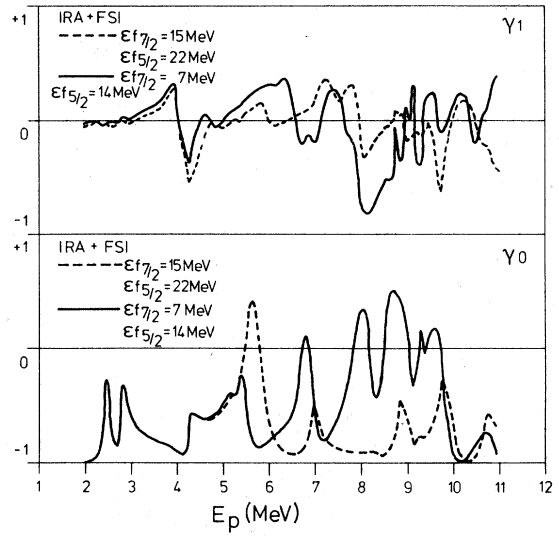

FIG. 12. The a_2 coefficients as obtained in the IRA + FSI approximation for the two different sets of $0f$-single-particle energies.

is rather good at least up to 7.5 MeV incident energy, the (p,γ_1) angular distribution is far off the experimental result. There may be two reasons for this discrepancy. The appearance of two peaks at around 6 MeV in the (p,γ_0) reaction instead of just one experimentally observed seems to indicate that the energies of Set II of states are probably a little too low, by about 1 MeV. In a different calculation where the $0f$ energies are shifted upward, the high energy part of the angular distributions seems to be improved (Fig. 12). Nevertheless, Set I is definitely too high to give enough strengths in the region where resonances are observed. The second reason may be due to the fact that we have neglected quadrupole transitions. This would involve intermediate states with $J^\pi = 0^+$, 1^+, 2^+, 3^+, and 4^+ for the (p,γ_1) reaction and probably would change markedly the angular distributions (though not necessarily the cross sections) for this reaction much more than for the (p,γ_0) reaction where only $J^\pi = 2^+$ would contribute.

The integrated total cross sections for the inverse reaction as obtained using the various approximations discussed above together with the experimental values are given in Table I. Set I does not give enough strength while the agreement with experiment for Set II is excellent, even though it has been enforced by our choice of $\Gamma_x = 150$ keV.

IV. CONCLUSION

In this work,[49] we have proposed a microscopic model for the description of the GMR in light deformed nuclei and their excitation via radiative capture reactions. In this model, the bound states of the A and $A-1$ nucleon systems are described as linear combinations of angular momentum projected p-h and h states in a deformed Hartree-Fock field. The angular momentum projections are performed exactly and furthermore are applied before the Hamiltonian is diagonalized. Spurious admixtures due to the center-of-mass motion are eliminated, at least approximately. The connection to the continuum is done using a version of Feshbach's formalism of nuclear reactions. Continuum and bound states are properly orthogonalized and furthermore defined in such a way that scattering waves will contain no single-particle resonance and hence the channel-channel coupling can be neglected.

The model has been applied to study the GMR in ^{20}Ne via the (p,γ) radiative reaction. Various approximations have been tested, and it has been shown that the isolated resonance approximation is not always valid, especially when intermediate states are densely populated as in the case of the (p,γ_1) reaction. The agreement of our theoretical results for the 90° yields with experiment is remarkably good, for both (p,γ_0) and (p,γ_1) reactions. Besides the gross features, most of the intermediate structures are also reproduced. Of course, the agreement is not yet completely satisfying. Improvements may be expected from the inclusion of the quadrupole transitions as well as from a careful choice of the effective interaction

TABLE I. Theoretical and experimental values for the integrated total (γ,p) cross sections.

Approximation	$\sum_{\gamma_0}$[MeV mb] $(0^+ \rightarrow 1^-)$	$\sum_{\gamma_1}$[MeV mb] $(2^+ \rightarrow 1^-, 2^-, 3^-)$	$\sum_{\gamma_2}$[MeV mb] $(4^+ \rightarrow 3^-)$
IRA + FSI (I)	21.38	4.22	0.25
IRA + FSI (II)	27.01	7.24	0.55
MIA (II)	24.08	6.22	0.43
MIA + FSI (II)	24.72	6.43	0.45
Experiment	24.81	9.57	•••

and single-particle energies. We believe, however, that the present work can already be considered as a meaningful step in the direction of a microscopic understanding of both the microscopic structure as well as the excitation mechanism of the GMR in light deformed nuclei.

One of us (K.W.S.) would like to acknowledge the kind hospitality of the Laboratoire de Physique Théorique et Hautes Energies at Orsay during his one year stay in 1975 and to thank Professor A. Faessler for helpful discussions. We have also benefitted from financial support from an exchange program between the Centre National de la Recherche Scientifique and the Deutsche Forschungsgemeinschaft.

*Laboratoire associé au Centre National de la Recherche Scientifique.

[1]H. E. Gove, A. E. Litherland, and R. Batchelor, Nucl. Phys. 26, 480 (1961).

[2]N. W. Tanner, G. C. Thomas, and E. D. Earle, Nucl. Phys. 52, 29 (1964).

[3]R. G. Allas, S. S. Hanna, L. Meyer-Schützmeister, R. E. Segel, P. P. Singh, and Z. Vager, Phys. Rev. Lett. 13, 628 (1964).

[4]R. G. Allas, S. S. Hanna, L. Meyer-Schützmeister, and R. E. Segel, Nucl. Phys. 58, 122 (1964).

[5]P. P. Singh, R. E. Segel, L. Meyer-Schützmeister, S. S. Hanna, and R. G. Allas, Nucl. Phys. 65, 577 (1965).

[6]R. E. Segel, Z. Vager, L. Meyer-Schützmeister, P. P. Singh, and R. G. Allas, Nucl. Phys. A93, 31 (1967).

[7]*Proceedings of the International Conference on Photonuclear Reactions and Applications, Asilomar*, 1973, edited by B. L. Berman (Lawrence Livermore Laboratory, Univ. of California, 1973).

[8]S. S. Hanna, in *Proceedings of the International Conference on Nuclear Structure Spectroscopy, Amsterdam*, 1973, edited by H. P. Blok and A. E. L. Dieperink (Scholar's Press, Amsterdam, 1974), Vol. 2, p. 249.

[9]S. S. Hanna, H. F. Glavish, J. R. Calarco, R. LaCanna, E. Kuhlmann, and D. G. Mavis, in *Proceedings of the International Symposium on Highly Excited States of Nuclei*, Jülich, 1975 (unpublished), Vol. 1, p. 8.

[10]M. N. Harakeh, P. Paul, and K. A. Snover, Phys. Rev. C 11, 998 (1975); M. N. Harakeh, P. Paul, and P. Gorodetzky, *ibid.* 11, 1008 (1975).

[11]P. Paul, in *Proceedings of the International Symposium on Highly Excited States of Nuclei*, Jülich, 1975 (see Ref. 9), Vol. 2 p. 72.

[12]J. P. Elliot and B. H. Flowers, Proc. R. Soc. A242, 57 (1957).

[13]G. E. Brown and M. Bolsterli, Phys. Rev. Lett. 3, 472 (1959).

[14]G. E. Brown, L. Castillejo, and J. A. Evans, Nucl. Phys. 22, 1 (1961).

[15]V. Gillet, and N. Vinh Mau, Nucl. Phys. 54, 321 (1964).

[16]R. H. Lemmer and C. M. Shakin, Ann. Phys. (N.Y.) 27, 13 (1964).

[17]B. Buck and A. D. Hill, Nucl. Phys. A95, 271 (1967).

[18]V. Gillet, M. A. Melkanoff, and J. Raynal, Nucl. Phys. A97, 631 (1967).

[19]J. Raynal, M. A. Melkanoff, and T. Sawada, Nucl. Phys. A101, 369 (1967).

[20]B. M. Spicer, Adv. Nucl. Phys. 2, 1 (1969).

[21]W. L. Wang and C. M. Shakin, Phys. Rev. C 5, 1898 (1972).

[22]J. Birkholz, Nucl. Phys. A189, 385 (1972).

[23]S. Krewald, J. Birkholz, A. Faessler, and J. Speth, Phys. Rev. Lett. 33, 1386 (1974).

[24]E. Grecksch, W. Knüpfer and M. G. Huber, Nuovo Cimento Lett. 14, 505 (1975).

[25]W. Knüpfer and M. G. Huber, Z. Phys. A (to be published).

[26]S. Krewald, V. Klemt, J. Speth, and A. Faessler, Nucl. Phys. (to be published).

[27]J. S. Dehesa, S. Krewald, J. Speth, and A. Faessler, Phys. Rev. C (to be published).

[28]I. R. Afnan, Phys. Rev. 163, 1016 (1967); see also G. Pisent and F. Zardi, Nuovo Cimento 48, 174 (1967).

[29]M. Maragoni and A. M. Saruis, Nucl. Phys. A166, 397 (1971).

[30]D. Zawischa and J. Speth, Phys. Rev. Lett. 36, 843 (1976).

[31]M. Danos, Nucl. Phys. 5, 23 (1958); K. Okamoto, Phys. Rev. 110, 143 (1958); M. Danos and E. G. Fuller, Annu. Rev. Nucl. Sci. 15, 29 (1965); M. Danos and W. Greiner, Phys. Lett. 8, 113 (1964).

[32]See, for example, E. G. Fuller and E. Hayward, Nucl. Phys. 30, 613 (1962); other references are listed in Ref. 20.

[33]A. Bohr and B. R. Mottelson, K. Dan. Vidensk. Selsk. Mat–Fys. Medd. 27, No. 16 (1953).

[34]Many-Body Description of Nuclear Structure and Reactions, in *Proceedings of the International School of Physics, "Enrico Fermi," Course XXXVI*, edited by C. Bloch (Academic, New York, 1966); C. Mahaux, and H. A. Weidenmüller, *Shell-Model Approach to Nuclear Reactions* (North-Holland, Amsterdam/American-Elsevier, New York, 1969).

[35]H. Feshbach, Ann. Phys. (N.Y.) 5, 357 (1958); 19, 287 (1962).

[36]E. P. Wigner, L. Eisenbud, Phys. Rev. 72, 49 (1947); A. M. Lane and R. G. Thomas, Rev. Mod. Phys. 30, 257 (1958); A. A. Ayad and D. J. Rowe, Nucl. Phys. A218, 307 (1974).

[37]K. W. Schmid and G. Do Dang, Z. Phys. A276, 233 (1976).

[38]J. P. Elliot and T. H. R. Skyrme, Proc. R. Soc. A323, 561 (1955).

[39]For example, G. Ripka, Adv. Nucl. Phys. 1, 183 (1968).

[40]F. Villars, Many-Body Description of Nuclear Structure and Reactions (see Ref. 34).

[41]A. Messiah, *Quantum Mechanics* (North-Holland, Amsterdam, 1969).

[42]B. Giraud, Nucl. Phys. 71, 373 (1965).

[43]R. H. Lemmer and M. Veneroni, Phys. Rev. 170, 883 (1968).

[44]N. Auerbach, J. Hüfner, A. K. Kerman, and C. M.

Shakin, Rev. Mod. Phys. 44, 48 (1972).
[45]W. L. Wang and C. M. Shakin, Phys. Lett. 32B, 421 (1970).
[46]K. W. Schmid, S. Krewald, A. Faessler and L. Satpathy, Z. Phys. 271, 149 (1974); S. Krewald, K. W. Schmid, A. Faessler and J. B. McGrory, Nucl. Phys. A228, 524 (1974).
[47]P. W. M. Glaudemans, P. J. Brussaard and B. H. Wildenthal, Nucl. Phys. A102, 593 (1967); E. Halpert, J. B. McGrory, B. H. Wildenthal, and S. P. Pandhya, Adv. Nucl. Phys. 4, 316 (1971).
[48]F. Ajzenberg-Selove, Nucl. Phys. A190, 1 (1972).
[49]Preliminary results have been reported earlier; K. W. Schmid and G. Do Dang, Jülich report, 1976 (unpublished).